

A microfluidic device for separation of amniotic fluid mesenchymal stem cells utilizing louver-array structures

Huei-Wen Wu · Xi-Zhang Lin · Shiaw-Min Hwang · Gwo-Bin Lee

Published online: 3 September 2009
© Springer Science + Business Media, LLC 2009

Abstract Human mesenchymal stem cells can differentiate into multiple lineages for cell therapy and, therefore, have attracted considerable research interest recently. This study presents a new microfluidic device for bead and cell separation utilizing a combination of T-junction focusing and tilted louver-like structures. For the first time, a microfluidic device is used for continuous separation of amniotic stem cells from amniotic fluids. An experimental separation efficiency as high as 82.8% for amniotic fluid mesenchymal stem cells is achieved. Furthermore, a two-step separation process is performed to improve the separation efficiency to 97.1%. These results are based on characterization experiments that show that this microfluidic chip is capable of separating beads with diameters of 5, 10, 20, and 40 μm by adjusting the volume-flow-rate ratio between the flows in the main and side channels of the T-junction focusing structure. An optimal volume-flow-rate ratio of 0.5 can lead to high separation efficiencies of 87.8% and 85.7% for 5- μm and 10- μm beads, respectively, in a one-step separation process. The development of this microfluidic chip may be promising for future research into stem cells and for cell therapy.

H.-W. Wu · G.-B. Lee (✉)
Department of Engineering Science,
National Cheng Kung University,
Tainan 701, Taiwan
e-mail: gwobin@mail.ncku.edu.tw

X.-Z. Lin
Department of Medicine, National Cheng Kung University,
Tainan 701, Taiwan

S.-M. Hwang
Bioresource Collection and Research Center, Food Industry
Research and Development Institute,
Hsinchu 300, Taiwan

Keywords Amniotic fluid · MSC · Separation · MEMS · Microfluidics

Nomenclature

AF	amniotic fluid
AFMSC	amniotic fluid mesenchymal stem cell
Bio-MEMS	bio-micro-electro-mechanical-systems
BCRC	Bioresource Collection and Research Center
CMOS	complementary-metal-oxide-semiconductor
DEP	dielectrophoretic
DIP	digital image processing
EOF	electroosmotic flow
FITC	fluorescein isothiocyanate
IgG	immunoglobulin G
MSC	mesenchymal stem cell
MEMS	micro-electro-mechanical-systems
ODEP	optically induced dielectrophoresis
PBS	phosphate buffered saline
PDMS	polydimethylsiloxane
PR	photoresist
RBC	red blood cell
SEM	scanning electron microscope
UV	ultraviolet
WBC	white blood cell

1 Introduction

Human mesenchymal stem cells (MSC) in adult tissues have the promising therapeutical potential to provide differentiated cells, which are extremely useful for tissue engineering or cell therapy (Hwang et al. 2008a). With their multi-potent beneficial characteristics, osteoblasts, adipo-

cytes, chondrocytes, astrocytes, neurons, and myoblasts can be differentiated from MSC *in vitro* and *in vivo* (Cipriani et al. 2007). These useful cells, capable of having either ectoderm, mesoderm or endoderm characteristics, can be derived from adult bone marrows (Jiang et al. 2007), cord bloods (Lee et al. 2004), placentas (Yen et al. 2005), and adipose tissues (Kang et al. 2003). Especially, the presence of MSC in amniotic fluid (AF) is an attractive cell source without ethical concerns when compared with the use of human embryonic stem cells (In 't Anker et al. 2003). Due to their availability, the therapeutic evaluation of amniotic fluid mesenchymal stem cells (AFMSC) have been extensively investigated recently (Rehni et al. 2007; Kolambkar et al. 2007; Siegel et al. 2008; Schmidt et al. 2007; Perin et al. 2007). It was reported that human MSC can be isolated from second-trimester AF with the capability to differentiate into multiple types of cells *in vitro* using a two-stage culture protocol (Hwang et al. 2008b). However, this requires a relatively complicated culture process, costly and bulky equipment, and experienced personnel to achieve reasonable separation efficiency (about 86%) (Chang et al. 1992). Therefore, there still remains a critical need to develop a fast, compact, cost-effective and automatic platform for AFMSC separation.

Recently, techniques using bio-micro-electro-mechanical-systems (Bio-MEMS) have been demonstrated as an enabling technology for cell separation. These techniques have many advantages over their large-scale counterparts, including miniaturized device size, high throughput, automation, and a short processing time. There are several Bio-MEMS approaches for cell separation. Typical mechanisms include hydrodynamic (Yang et al. 2006; Yang et al. 2008), electrokinetic (Chien et al. 2006), dielectrophoretic (Gascoyne et al. 1992; Han and Frazier 2008; Pommer et al. 2008; Barrett et al. 2005; Barbulovic-Nad et al. 2006; Ohta et al. 2007; Lin and Lee 2008), magnetic (Rong et al. 2006; Lin et al. 2007), a combination of gravity and hydrodynamic forces (Li et al. 2007), acoustic (Huh et al. 2007), laminar flow control (Laurell et al. 2007; Xia et al. 2006; Yamada et al. 2004; Sai et al. 2006; Wu et al. 2007) and microfiltering approaches (Yamada and Seki 2005; Choi et al. 2007; Wilding et al. 1998; Sethu et al. 2006). For instance, microfluidic-based flow cytometers fabricated by micromachining techniques have been extensively studied and used for cell sorting and separation (Yang et al. 2006; Yang et al. 2008). In these devices, basically, neighboring sheath flows with a higher velocity hydrodynamically squeeze a central flow containing fluorescence-labeled cells into a narrow stream. When they pass an optical detection area, fluorescence emission due to laser excitation from the cells is then detected and then the cells are sorted and separated to the appropriate subsequent collectors. Similarly, a digital image projection technique

(DIP) using optical tweezers capable of catching and switching the target cells under a microfluidic configuration has been reported to electrokinetically sort and separate beads or cells (Chien et al. 2006).

Besides, a variety of sorting devices using dielectrophoretic (DEP) forces was reported to be promising for cell separation (Gascoyne et al. 1992; Han and Frazier 2008; Pommer et al. 2008). When an inhomogeneous electric field exists, polarized cells will move due to the induced dipole. Obstacles such as ridges and wedges embedded in the microchannel can be used to generate the inhomogeneous electric field. However, these obstacles may result in serious clogging of the channel. Recently, a microfluidic device was presented using a virtual, projected pillar array to induce a negative DEP force, thus eliminating the clogging issue (Barrett et al. 2005; Barbulovic-Nad et al. 2006). Alternatively, an optically-induced dielectrophoresis (ODEP) device can be used to generate various types of virtual microelectrodes to manipulate beads and cells (Ohta et al. 2007). With this approach, there is no need to fabricate microelectrodes and beads or cells can be manipulated and separated. For example, an optically-induced flow cytometer for continuous bead and cell counting and sorting using ODEP has been reported by our group recently (Lin and Lee 2008). Alternatively, a micromachined magnetic separator for cell sorting in microfluidic systems has been presented (Rong et al. 2006). Its flexible design utilized fully integrated electromagnetic inductors that are placed underneath the device chip. Similarly, a micro device using an inhomogeneous magnetic field perpendicular to the direction of the flow such that beads/cells of different sizes can be separated was also reported (Lin et al. 2007). Similarly, living *E. coli* bacteria bound onto magnetic nanoparticles can be separated in a continuous laminar flow by applying a local magnetic field gradient (Li et al. 2007). On the other hand, a microfluidic sorter utilizing a combination of gravity and hydrodynamic forces was demonstrated for continuous mass-dependent separation of cells (Huh et al. 2007). Acoustic forces generated from ultrasonic waves can be also used to sort cells (Laurell et al. 2007). Bioparticles can also be concentrated by using an asymmetric surface acoustic wave method (Xia et al. 2006). However, such systems mentioned above always require complicated fabrication processes or costly equipment. Furthermore, cell samples may be damaged when applying external forces.

Recently, simple methods using the benefits of a laminar flow have been reported for cell separation (Yamada et al. 2004; Sai et al. 2006; Wu et al. 2007). For instance, microfluidic devices using the concept of pinched flow fraction for continuous cell separation has been demonstrated, and red blood cells (RBCs) were successfully

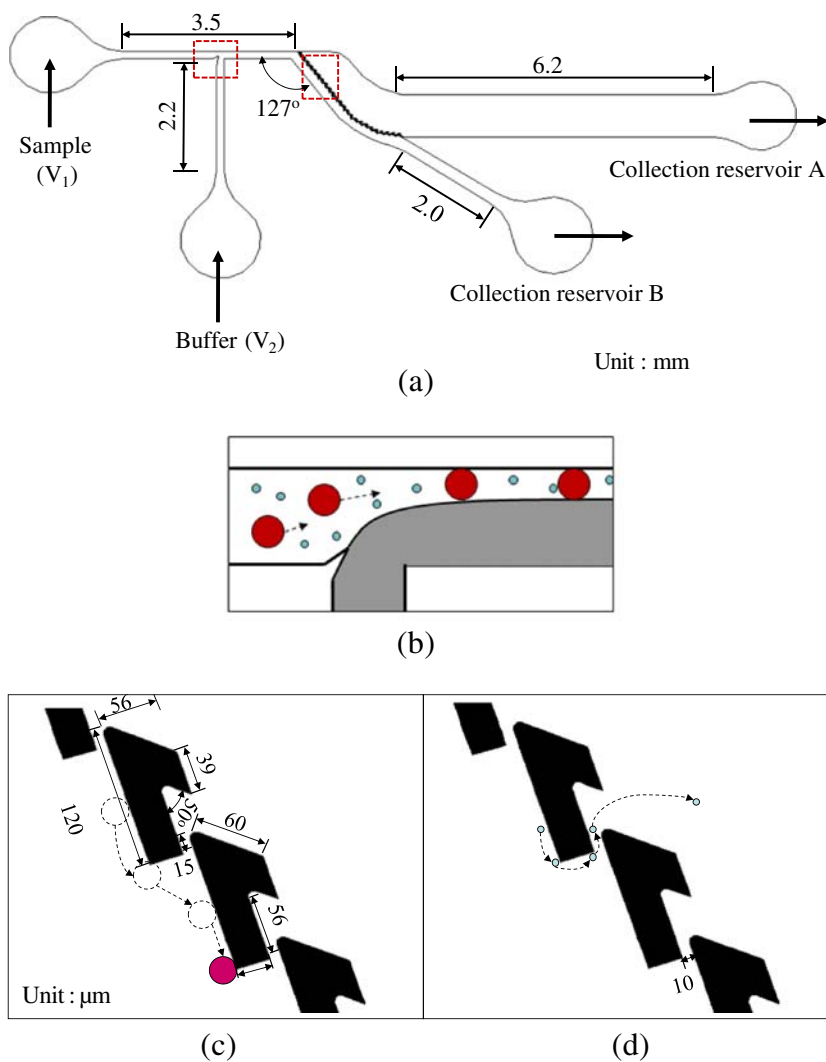
separated from human whole blood (Yamada et al. 2004; Sai et al. 2006). An integrated device using a combination of an electroosmotic flow (EOF) and a pinched flow for separation of *E. coli* and yeast cells was also demonstrated (Wu et al. 2007). Alternatively, based on flow control and microchannel design, cell separation can be also performed by hydrodynamic filtration (Yamada and Seki 2005; Choi et al. 2007). For example, the enrichment of leukocytes from blood was successfully performed (Yamada and Seki 2005). Similarly, a microfluidic device composed of slanted obstacles was reported for continuous blood cell separation (Choi et al. 2007). Successful isolation of white blood cells (WBCs) with 210-fold enrichment can be achieved.

Even though these devices can be used for cell separation, they require precise fluid control to attain higher separation efficiencies. To solve this problem, microfilters with different geometries have been inserted into the microchannels, with the advantage of simplified operation (Wilding et al. 1998). For example, a microfluidic diffusive

filter for leukapheresis, which is the isolation of red blood cells and plasma from blood, was demonstrated (Sethu et al. 2006). Similarly, a separator for isolating WBCs from human whole blood was designed using a cross-flow method in an array of microchannels (Delinder and Groisman 2007). The fraction of WBCs was enriched about 4000 fold in a single passage using that device. Another silicon-based microfilter for white blood cell separation was also presented (Ji et al. 2008). The cross-flow microfilter was reported to have an average separation efficiency of 70–80% in trapping WBCs. Nevertheless, the issue regarding fouling of the microchannels still needs to be addressed properly.

In this study, a new cell separation chip was reported. The cells are successfully isolated by a combination of a T-junction focusing structure and louver-like structures embedded as a microfilter, which allow the target cells to flow through and unwanted larger cells to flow away from the tilted channel due to hydrodynamic forces. Therefore,

Fig. 1 **a** Schematic illustration of the cell separation chip; **b** Detailed view showing that beads or cells can be focused to form a narrow stream; (c) and (d) Detailed dimensions of the chip and cell separation mechanism. **c** The larger beads or cells are separated by the louver-like structures; **d** The smaller beads or cells flow through the gap between the louver-like structures



the fouling issue is solved successfully and the cells remain intact due to the lack of a large external force during the separation process. Experimental results show that a relatively high separation efficiency can be achieved. To the best of the authors' knowledge, this is the first time that a microfluidic device is capable of continuous separation of amniotic stem cells.

2 Materials and methods

2.1 Chip design

A schematic diagram of the microfluidic chip is shown in Fig. 1(a). It is composed of one sample inlet, one buffer inlet, two collection reservoirs, a sample flow channel, a buffer flow channel and 24 louver-like filtering structures. As shown in Fig. 1(a), the angle of inclination of the louver-like structure channel is 130° , which is designed to induce a laminar flow. The angle between two collection channels is 30° . The length of the sample flow channel and the buffer flow channel are 3.5 mm and 2.2 mm, respectively. The width and the depth of these two channels are $150\ \mu\text{m}$ and $50\ \mu\text{m}$, respectively. With this design, a buffer solution injected into the buffer flow channel is used to squeeze the sample flow to form a narrow stream so that the cells can be pushed closer to the louver-like structures to obtain a higher separation efficiency. This is schematically illustrated in Fig. 1(b). Moreover, a sharp corner structure close to the intersection of the sample and buffer flow channels is used to enhance the focusing effect (Lin et al. 2006). With this approach, the cells can be squeezed more efficiently to form a narrower stream and can improve the cell separation in the following separation process. The louver-like structure has a gap of $10\ \mu\text{m}$ and a depth of $50\ \mu\text{m}$ (Fig. 1(d)). It is used as a microfilter such that amniotic stem cells with a diameter of $4\text{--}6\ \mu\text{m}$ can be separated from AFs and collected in the collection reservoir A. This unique structure also allows larger cells to flow downwards instead of clogging the gap. The distances between the louver-like filtering structures and the collection reservoir A and B are 5.8 mm and 2.0 mm, respectively. The widths of these two channels are $900\ \mu\text{m}$ and $210\ \mu\text{m}$, respectively.

The flow and sorting mechanism for cells with different sizes is depicted in Figs. 1(c) and (d). The main mechanism is physical separation of particles/cells based on blocking the objects. However, in this study, a louver-like structure was adopted to cleverly direct particles to flow through or along the structure. It is the combination of the three two effects such that a high separation efficiency can be achieved. When the volume flow ratio (V_1/V_2) becomes smaller, more small particles pass through the filter because

the particle flow can be pushed closer toward the gap by the larger velocity of the buffer flow. Therefore, the separation efficiency of small particles can be improved by controlling the volume flow ratio, which has been already described in the original manuscript. It has been observed that if particles are not pre-focused to flow along the louver-like structures, then a great portion of small particles will not pass through the gap, which is quite different from pure "size-exclusion" filter. For large particles, when they leave the corner of the first louver, they hit the long side of the second louver and cannot flow through the gap between the louvers (Fig. 1(c)). As a result, they flow along the long sides of the louver-like structures and finally are collected in the collection reservoir B. Note that the length and width of the louver is $120\ \mu\text{m}$ and $60\ \mu\text{m}$, respectively.

2.2 Fabrication process

The microfluidic chip is fabricated using a MEMS process by constructing elastic PDMS structures on a glass substrate. Using a standard lithography and a two-step

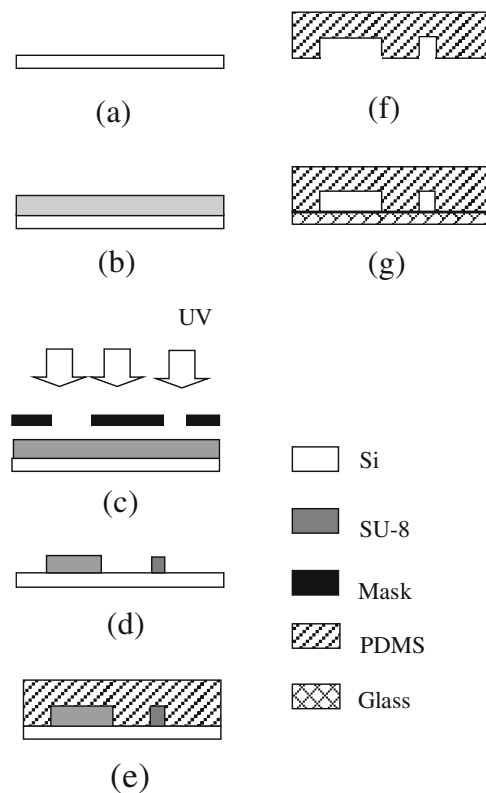
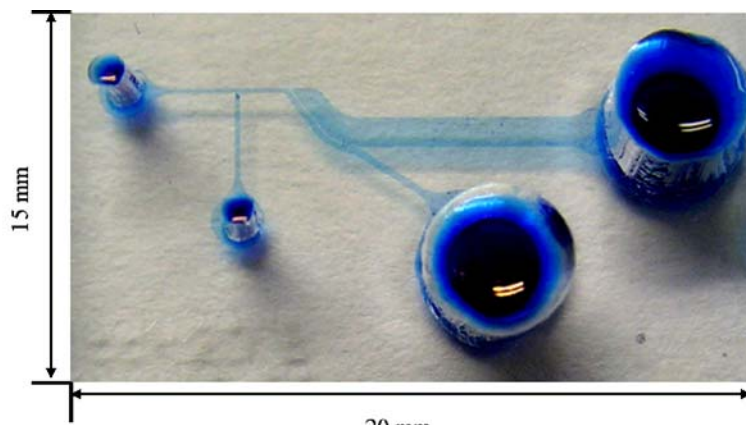


Fig. 2 Schematic illustration of the fabrication process for the cell separation chip. **a** a silicon wafer is cleaned; **b** SU-8 negative thick PR is spin-coated onto the silicon wafer; **c–d** A standard lithography process is used to form the SU-8 mold structures; **e** PDMS is poured on the SU-8 microstructure mold; **f** PDMS inverse structures are formed and mechanically peeled off the mold; **g** An oxygen plasma treatment is performed prior to bonding the PDMS layers and glass substrate to form the chip

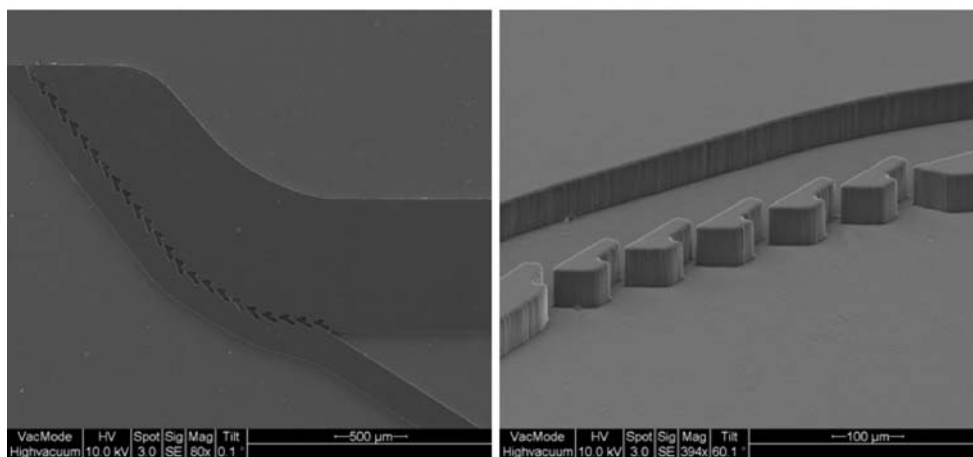
photoresist baking processes, a SU-8 master mold is formed and is used to replicate the PDMS structure (Wang and Lee 2006). Figure 2 shows a simplified fabrication process using the SU-8 master mold and the replication process of the PDMS structure. Briefly, SU-8 (50) (NANO®, MicroChem,

USA) negative thick photoresist (PR) is spin-coated on a silicon wafer to form a 50- μm thick layer SU-8 mold. Then a two-step, soft baking process on a hotplate is performed at 65°C for 6 min and then at 95°C for 20 min. An exposure dose of 250 mJ/cm² is performed in a standard lithography

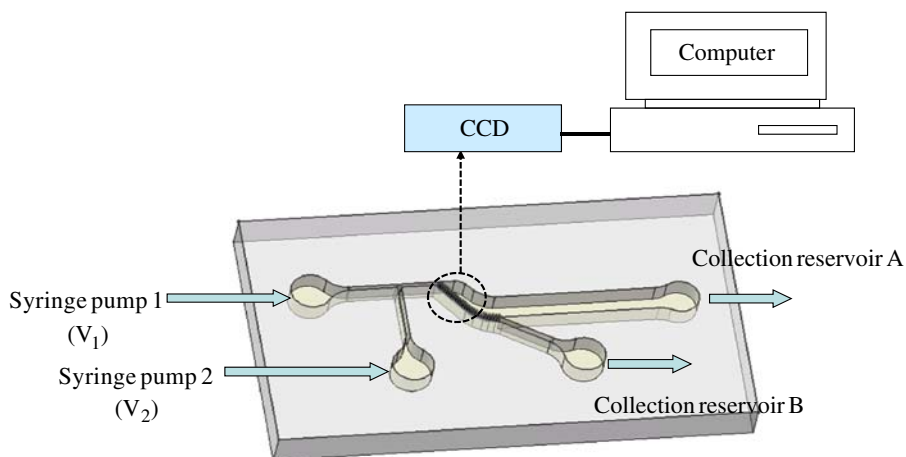
Fig. 3 **a** A photograph of an assembled microfluidic chip. The dimensions of the chip are measured to be 15 mm and 20 mm in width and length, respectively; **b** SEM images of the SU-8 structure and the PDMS mold of the microchip structures. **c** The experimental setup which is used for the separation of beads and AFMSCs. It is composed of an optical microscope, a CCD and two syringe pumps



(a)



(b)



(c)

process. A post-exposure baking process is then conducted at 65°C for 1 min and then at 95°C for 5 min, followed by using ultrasonic agitation with a SU-8 developer solution to release the SU-8 mold. Finally, a thick PDMS layer of 500 μm is formed using the casting process and is bonded with a glass substrate by using an oxygen plasma treatment. Figure 3(a) is a photograph of the microfluidic chip. The dimensions of the chip are measured to be 20 mm in length and 15 mm in width. SEM images of the SU-8 structure and the PDMS mold of the louver-like structures are also shown in Fig. 3(b).

2.3 Experimental setup

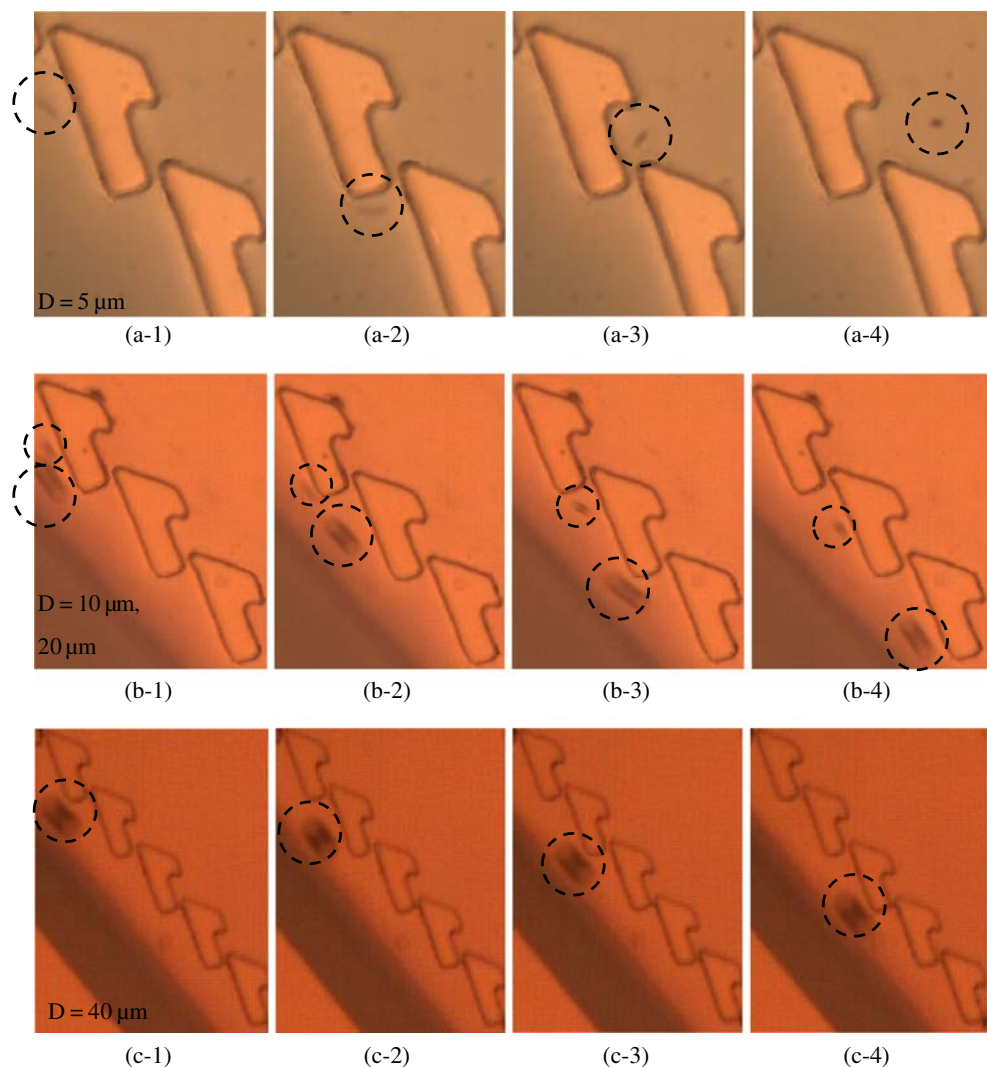
Figure 3(c) illustrates the experimental setup for the bead/cell separation. It consists of an optical microscope (TE300, Nikon, NY, USA), a high-speed complementary-metal-oxide-semiconductor (CMOS) camera (MC 1311, Microtron, Germany), and two syringe pumps (KD Scientific Inc.,

KDS200, MA, USA). Typically, phosphate buffered saline (1X) (PBS, Merk Ltd., Germany) is used as the buffer solution for the separation experiments of the beads and the cells. Two syringe pumps are used to inject the bead or cell sample solution and the buffer solution into the microfluidic chip. The sample flow is then squeezed into a narrow stream to achieve a higher separation efficiency. Beads or cells collected in the collection reservoirs are observed under an optical microscope and recorded by a computer equipped with a CCD device. For beads, after collecting them into an Eppendorf tube, a flow cytometer (BD FACSCalibur Flow Cytometer, BD Biosciences, USA) is used to count the number of the beads. For amniotic stem cells, they are counted by immunofluorescence staining, as described in the following section.

2.4 MSCs immunofluorescence staining assay

Amniotic fluids are provided from the cell bank of the Bioresource Collection and Research Center (BCRC) in

Fig. 4 CCD images marking the path of beads with various diameters while the chip is operated at a volume-flow-rate ratio of 0.5. **a** and **c**: sample solutions with 5- μm and 40- μm beads only; **b** a mixture of 10- and 20- μm beads



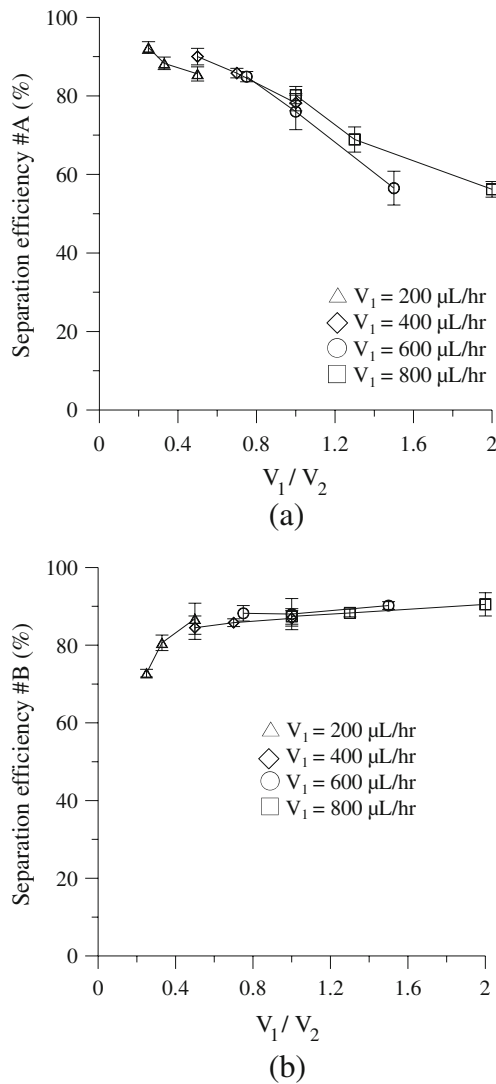


Fig. 5 Relationship between the separation efficiency of the beads and the sample/buffer volume-flow-rate ratio. The sizes of the beads are **a** 5 μm and **b** 10 μm , respectively

Taiwan. The number of AFMSC cells is estimated to be 2.4×10^3 in every 20- μl AF for the separation experiment. After separating AFMSCs, the collected MSCs are then observed by using immunofluorescence staining, as described as follows. The primary antibody 1:50 dilution of CD105 (abcame, UK) is first added into the collected cells and is shaken for 40 min using a large-scale shaker (INTELLIMIXER, ELMI Ltd, Latvia) at room temperature. After washing them twice with PBS, the cells are mixed with a second antibody, an 1: 50 dilution of anti-mouse immunoglobulin G (IgG) conjugated with fluorescein isothiocyanate (FITC, abcame, UK). After shaking for 30 min, PBS is twice used to wash the chip. Then the cells are taken off of the chip and are then observed and counted using a counter under a fluorescence microscope.

3 Results and discussion

3.1 Bead separation

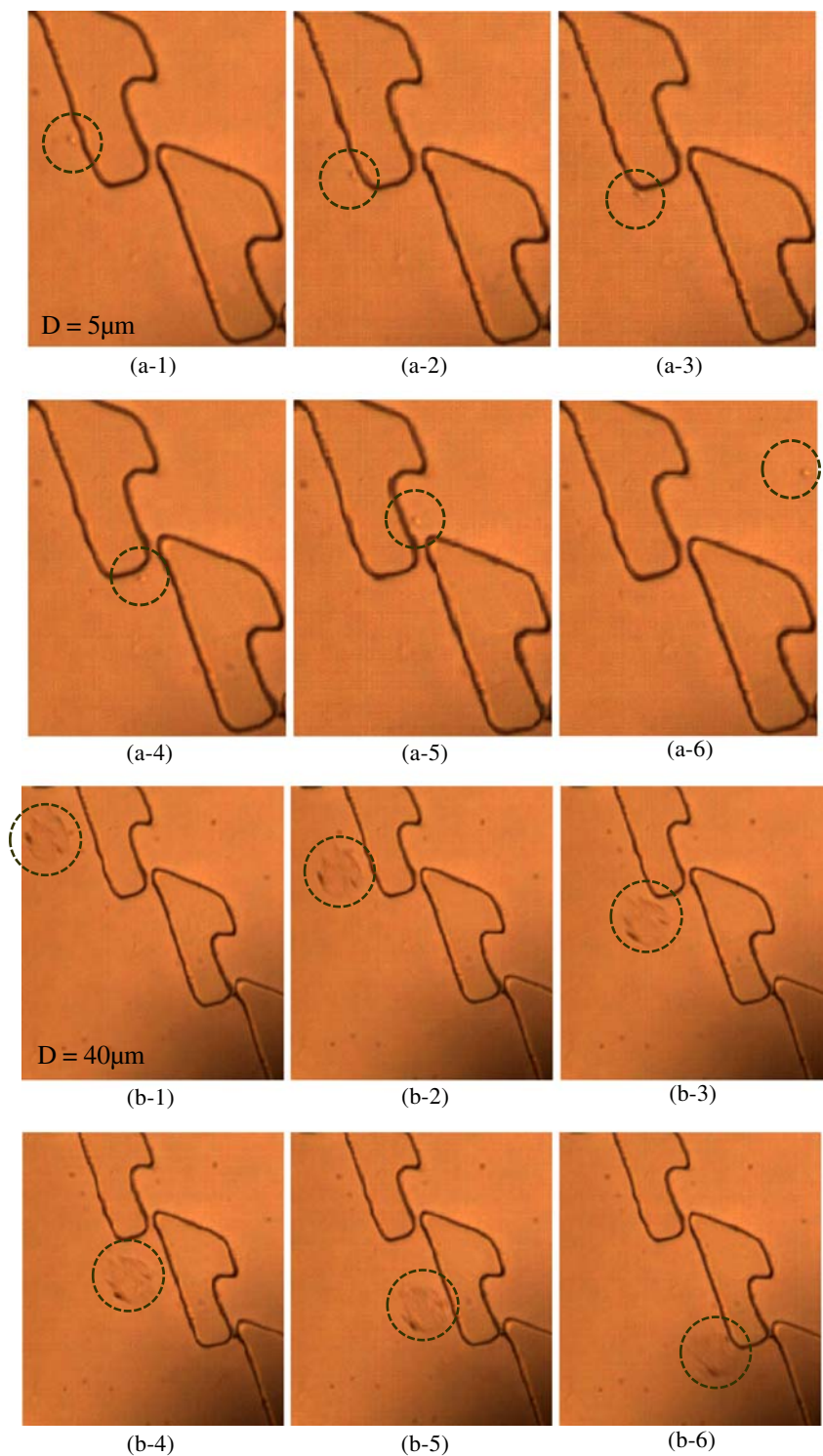
The purpose of the designed chip is to separate amniotic stem cells with a size of 4–6 μm from AFs. In order to optimize the operating conditions, different-size beads are first tested using the developed chip. Figure 4 shows a series of CCD images indicating that beads with various sizes are flowing close to the louver-like structures. The diameters of these beads are 5, 10, 20, and 40 μm , respectively, and the chip is operated at a constant volume-flow-rate ratio of 0.5 ($V_1=400 \mu\text{L/hr}$, $V_2=800 \mu\text{L/hr}$). In the first and third experiments (Figs. 4(a) and (c)), sample solutions with only 5- μm and 40- μm beads are used. For the second experiment (Fig. 4(b)), a mixture of 10- and 20- μm beads are used. From these images, it is clearly seen that 5- μm beads can successfully flow through the gap, as expected (Fig. 4(a)). The 10-, 20-, and 40- μm beads all flow downwards to the collection reservoir B. More importantly, they do not foul the filters (Figs. 4(a)~(c)). For a mixture with 10- and 20- μm beads, it is observed that the 20- μm beads pass over the 10- μm ones when they hit the louver and then move far away from it (Fig. 4(b)). This indicates that the larger beads are effectively separated by these louver-like structures.

The separation efficiency of beads is primarily determined by the volume-flow-rate ratio of the sample and the buffer flows. Another experiment is then performed to investigate this effect. A mixture of 5- μm and 10- μm beads, both with a count of 1×10^4 (200- μl in volume) is injected into the sample channel. Then the separation efficiency of the 5- μm beads is calculated by counting the number of the appropriate beads in the collection reservoir A and B. Note that the “separation efficiency #A” is defined as the ratio between the separated beads from collection reservoir A and total amount of the beads from collection reservoir A and B ($A/(A + B)$). The separation efficiency #A for the 5- μm beads at different operation conditions are shown in Fig. 5 (a). Four sample volume flow rates (V_1), specifically 200 $\mu\text{L/hr}$, 400 $\mu\text{L/hr}$, 600 $\mu\text{L/hr}$, and 800 $\mu\text{L/hr}$, respectively, are tested. For each case, the buffer volume flow rates (V_2) are fine-tuned to provide a volume-flow-rate ratio (V_1/V_2) ranging from 0.2 to 2.0. The elapsed times for each experiment are 60, 30, 20, and 15 min, respectively. For all cases with a fixed sample volume flow rate (V_1), it is observed that a higher separation efficiency is achieved

Table 1 The separation efficiency of beads with various diameters

Diameter (μm)	20	15	10
Separation efficiency (%)	100%	100%	>73%

Fig. 6 CCD images tracing the movement of amniotic cells: **a** an amniotic stem cell ($5\ \mu\text{m}$) **b** a larger cell ($40\ \mu\text{m}$)



when a higher buffer volume flow rate (V_2) is used, indicating that higher buffer volume flow rate focuses the sample flow efficiently into a narrower stream so that the beads can be pushed closer to the filter for better separation performance. Correspondingly, the experimental results also show that a lower volume-flow-rate ratio (V_1/V_2) results in higher separation efficiency. A high separation efficiency of

approximately 92.3% is achieved at a volume-flow-rate ratio of 0.25. Similarly, the relationship between the separation efficiency of the $10\text{-}\mu\text{m}$ beads and the volume-flow-rate ratio is presented in Fig. 5(b). The separation efficiency of $10\text{-}\mu\text{m}$ beads (called “separation efficient #B”) is defined as the ratio between the separated beads from collection reservoir B and total amount of the beads from collection reservoir A and B

($B/(A + B)$). Compared with Fig. 5(a), the results show that a higher separation efficiency is achieved at higher volume-flow-rate ratios. It is reasonable since 10- μm beads move very close to the louver-like structures and may go through the gap at lower volume-flow-rate-ratios. Even though the developed microfluidic device provides a high separation efficiency of 92.3% for 5- μm beads at a volume-flow-rate ratio of 0.25, the 10- μm beads just have a low separation efficiency of 72.8% at this flow condition. Therefore, a volume-flow-rate ratio of 0.5 is then chosen for the subsequent AFC separation, which has a separation efficiency of 87.8% for 5- μm beads and 85.7% for 10- μm beads. Note that the counting error is less than 6%.

A bead with a diameter R moving at a velocity v through a fluid of density ρ and viscosity μ is subject to an inertial

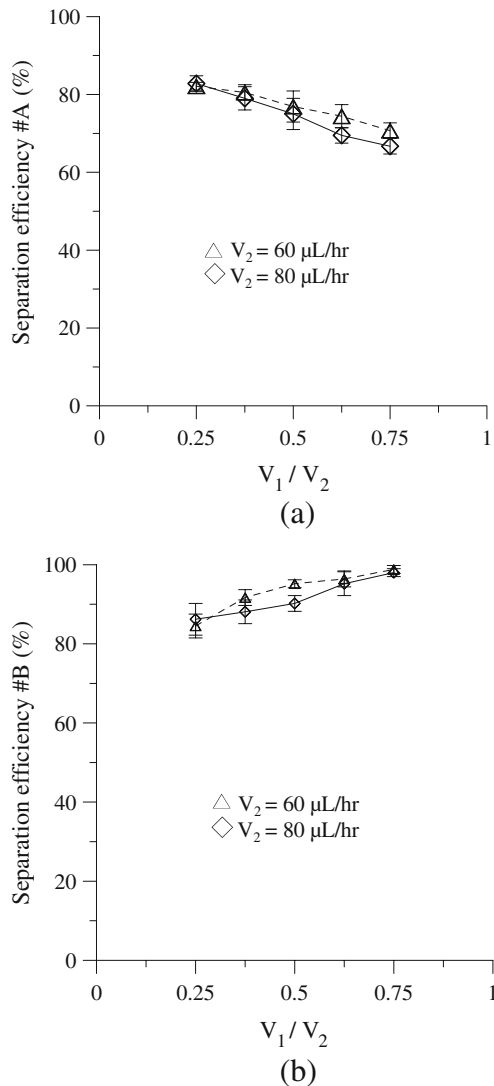


Fig. 7 Relationship between the separation efficiency of amniotic cells and the sample/buffer flow velocity ratio with two cells: **a** amniotic stem cells; **b** larger cells

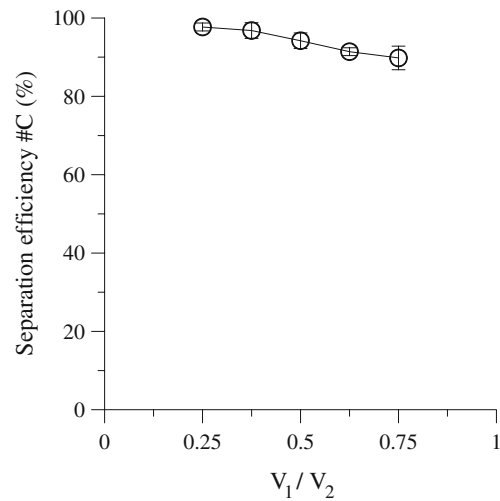


Fig. 8 Relationship between the separation efficiency of amniotic cells and the sample/buffer flow velocity ratio using a two-step separation process

force and a viscous drag force (Robert and Nanomedicine 1999). The inertial force is proportional to $\rho v^2 R^2$, and the viscous drag force is proportional to $\mu v R$. The ratio of inertial to viscous forces is usually referred to as the Reynolds number ($Re = \rho v R / \mu$). The Re is then calculated with $R = 5 \mu\text{m}$, $\rho = 1000 \text{ kg/m}^3$, $\eta = 10^{-3} \text{ kg/m-sec}$, for various velocities, as shown in Fig. 7. The widths of the buffer flow channel and the sample channel are both 150 μm . The width of the channel for louver-like structure is 210 μm and the depth of the channels is 50 μm . Therefore, the flow velocity, v , is calculated to be 0.026 m/s, 0.042 m/s, and 0.031 m/s at volume flow-rate-ratios of 200:800, 800:800, and 800:400, respectively. From these data, Re is then calculated to be 0.13, 0.21 and 0.16, respectively. For $Re < 1$, a “creeping flow” phenomenon makes the 5- μm beads flow along the louver structure and pass through the filter (Dhananjay et al. 2007). Similar to the above experiments, the separation efficiencies for 10-, 20-, and 40- μm beads (mixed with 5- μm beads) are listed in Table 1, respectively. Note that 1×10^4 beads are suspended in 200- μl water. The density and viscosity of water are 1000 kg/m^3 and 10^{-3} kg/m-sec , respectively. The data show that all beads larger than 15 μm can be completely separated by this chip. For 10- μm beads, the separation efficiency is higher than 73% for all operating conditions. It reaches 85.7% when the volume-flow-rate ratio is 0.5. These data indicate that some 10- μm beads can be squeezed through the gap. The separation efficiency can be improved by using a two-stage process to re-inject the collected sample through the louver-like structures again. Compared to other microfluidic systems for cell separation, this developed device provides a simple and passive approach to isolate the stem cells with high efficiency.

The simple method also solves the fouling problem that other devices may encounter.

3.2 Amniotic stem cell separation

There are a variety of cells in the AF. Most of them consist of stem cells, amniotic cells, and many dead epithelial cells with the corresponding diameter of 4–6 μm , 15–20 μm , and 40–60 μm , respectively. The developed chip is then used to separate amniotic stem cells from the AFs. An AF with 2.4×10^3 AFMSC in a volume of 20 μl is used. First, a series of CCD images are captured, as shown in Fig. 6. The volume-flow-rate ratio for this case is 0.5 ($V_1=40$ $\mu\text{L/hr}$, $V_2=80$ $\mu\text{L/hr}$). Since the cells are softer structurally compared to beads and may be squeezed through the gap of the louver-structure, both of the volume flow rates are reduced by one-tenth of their value in the previous experiments for bead separation. From these images, it can be clearly seen that stem cells (about 5 μm) can flow through the gap of the louver-structure successfully (Fig. 6 (a)) and the larger endothelial cells (about 40 μm) can be blocked (Fig. 6(b)).

Moreover, in order to quantify the separation efficiency, AFMSCs, are immunofluorescence-stained and counted. The relationship between the separation efficiency of the cells (MSCs and larger cells) and the volume flow rate ratio is shown in Fig. 7. Since an optimal value of 0.5 ($V_1 : V_2 = 400 : 800$) is determined from the bead separation, five ratios (0.25, 0.375, 0.5, 0.625, and 0.75) are tested to optimize the separation efficiency for AFMSCs. Two buffer volume flow rates (60 $\mu\text{L/hr}$ and 80 $\mu\text{L/hr}$) are tested. For all tests, the elapsed time is less than 60 min. The experimental results show that a lower volume-flow-rate ratio can result in a higher separation efficiency for AFMSCs. At different buffer volume flow rates, this same trend is observed. It is consistent with the results from bead separation. At a volume-flow-rate ratio of 0.25, the separation efficiency of AFMSCs is as high as 82.8%. The separation efficiency of the large cells is 84.9% at this condition as shown in Fig. 7(b). Note that the counting error is less than 6%. This separation efficiency is comparable to the traditional method (about 86%) (Chang et al. 1992). However, the developed method is a simple and fast method for automatic AFMSC separation.

Furthermore, as mentioned previously, a two-step separation process can be used to enhance the separation efficiency. After the first separation process, the cells in the collection reservoir A are pipetted for a second separation. The experimental results are shown in Fig. 8. For this test, the “separation efficiency # C” is defined as the ratio between the MSCs collected from reservoir A in two steps and the total amount of MSCs collected from reservoir A and B in the first step. Since similar results at

two buffer volume flow rates (60 $\mu\text{L/hr}$ and 80 $\mu\text{L/hr}$) are observed (as shown in Fig. 7), only the data for the condition at a buffer volume-flow-rate of 80 $\mu\text{L/hr}$ are shown here. Again, five volume-flow-rate ratios (0.25, 0.375, 0.5, 0.625, and 0.75) are tested. A high separation efficiency #C of 97.1% at a volume-flow-rate ratio of 0.25 is achieved. As a result, the highly efficient isolation of MSCs using a two-step process can be realized. Furthermore, no cell damage has been observed. This developed microfluidic chip has great potential to simplify stem cell separation and to further cell therapy.

4 Conclusions

The current study has demonstrated a microfluidic chip using a T-junction focusing device and tilted louver-like structures for stem cell separation. Beads with different sizes are first used to characterize the performance of the developed chip. Compared with other microfluidic devices employing similar techniques, a high separation efficiency is realized by injecting a large number of cell samples into the developed chip. No fouling of the system has been observed. The experimental results show that a separation efficiency as high as 82.8% for AFMSCs can be achieved. Furthermore, the separation process can be repeated to improve the separation efficiency to 97.1%. The development of this microfluidic chip may become a promising fundamental tool for the stem cell research and cell therapy.

Acknowledgements The authors gratefully acknowledge the financial support provided to this study by the National Science Council in Taiwan (NSC 97-2120-M-006-007). This work is also partially supported by the Ministry of Education, Taiwan, R.O.C. under the NCKU Project of Promoting Academic Excellence & Developing World Class Research Centers.

References

- I. Barbulovic-Nad, X.C. Xuan, J.S.H. Lee, D.Q. Li, *Lab. Chip.* **6**, 274 (2006)
- L.M. Barrett, A.J. Skulan, A.K. Singh, E.B. Cummings, G.J. Fiechtner, *Anal. Chem.* **77**, 6798 (2005)
- I.K. Chang, A. Tajima, Y. Yasuda, T. Chikamune, T. Ohno, *Cell Bio. Int. Rep. Sep.* **16**, 853 (1992)
- Y.S. Chien, C.H. Lin, F.J. Kao, C.W. Ko, *Mater. Sci. Forum.* **505–507**, 643 (2006)
- S. Choi, S. Song, C. Choi, J.K. Park, *Lab. Chip.* **7**, 1532 (2007)
- S. Cipriani, D. Bonini, E. Marchina, I. Balgkouranidou, *Cell Biol. Int.* **31**, 845 (2007)
- V.V. Delinder, A. Groisman, *Anal. Chem.* **79**, 2023 (2007)
- D. Dhananjay, S.G. Shelley, C.P. Daniel, T.A. Hatton, S.D. Patrick, *Lab. Chip.* **7**, 818 (2007)
- P.R.C. Gascoyne, Y. Huang, R. Peting, J. Vykoukal, F.F. Becker, *Meas. Sci. Technol.* **3**, 439 (1992)
- K.H. Han, A.B. Frazier, *Lab. Chip.* **8**, 1079 (2008)

- D. Huh, J.H. Bahng, Y. Ling, H.H. Wei, O.D. Kripfgans, J.B. Fowlkes, J.B. Grotberg, S. Takayama, *Anal. Chem.* **79**, 1369 (2007)
- S. Hwang, S. Varghese, J. Elisseeff, *Adv. Drug. Deliver. Rev.* **60**, 199 (2008a)
- S. Hwang, S. Varghese, J. Elisseeff, *Adv. Drug. Deliver. Rev.* **60**, 199 (2008b)
- P.S. In 't Anker, S.A. Scherjon, C. Kleijburg-van der Keur, W.A. Noort, F.H. Claas, R. Willemze, *Blood* **102**, 1548 (2003)
- H.M. Ji, V. Samper, Y. Chen, C.K. Heng, T.M. Lim, L. Yobas, *Biomed. Microdevices.* **10**, 251 (2008)
- Y. Jiang, B.N. Jahagirdar, R.L. Reinhardt, R.E. Schwartz, C.D. Keene, X.R. Ortiz-Gonzalez, M. Reyes, T. Lenvik, T. Lund, M. Blackstad, J. Du, S. Aldrich, A. Lisberg, W.C. Low, D.A. Largaespada, C.M. Verfaillie, *Nature* **447**, 880 (2007)
- S.K. Kang, D.H. Lee, Y.C. Bae, H.K. Kim, S.Y. Baik, J.S. Jung, *Exp. Neurol.* **183**, 355 (2003)
- Y.M. Kolambkar, A.A. Peister, A.S. Soker, A. Atala, R.E. Guldborg, *J. Mol. Hist.* **38**, 405 (2007)
- T. Laurell, F. Petersson, A. Nilsson, *Chem. Soc. Rev.* **36**, 492 (2007)
- O.K. Lee, T.K. Kuo, W.M. Chen, K.D. Lee, S.L. Hsieh, T.H. Chen, *Blood* **103**, 1669 (2004)
- H. Li, J. Friend, L. Yeo, *Biomed. Microdevices.* **28**, 4098 (2007)
- Y.H. Lin, G.B. Lee, *Biosens. Bioelectron.* **24**, 572 (2008)
- C.H. Lin, C.Y. Lee, L.M. Fu, 19th IEEE International Conference on Micro Electro Mechanical Systems (2006)
- Y.A. Lin, T.S. Wong, U. Bhardwaj, J.M. Chen, E. McCabe, C.M. Ho, *J. Micromech. Microeng.* **17**, 1299 (2007)
- A.T. Ohta, P.Y. Chiou, T.H. Han, J.C. Liao, U. Bhardwaj, E.R.B. McCabe, F. Yu, R. Sun, M.C. Wu, *J. Microelectromech. S.* **16**, 491 (2007)
- L. Perin, S. Giuliani, D. Jin, S. Sedrakyan, G. Carraro, R. Habibian, D. Warburton, A. Atala, R.E.D. Filippo, *Cell Prolif.* **40**, 936 (2007)
- M.S. Pommer, Y. Zhang, N. Keerthi, D. Chen, J.A. Thomson, C.D. Meinhart, H.T. Soh, *Electrophoresis* **29**, 1213 (2008)
- A.K. Rehni, N. Singh, A.S. Jaggi, M. Singh, *Behav. Brain Res.* **183**, 195 (2007)
- A.F.J. Robert, *Nanomedicine I.* (1999)
- R. Rong, J.W. Choi, C.H. Ahn, *J. Micromech. Microeng.* **16**, 2783 (2006)
- Y. Sai, M. Yamada, M. Yasuda, M. Seki, *J. Chromatogr. A.* **1127**, 214–220 (2006)
- D. Schmidt, J. Achermann, B. Odermatt, C. Breymann, A. Mol, M. Genoni, G. Zund, S.P. Hoerstrup, *Circulation* **116**, I-64 (2007)
- P. Sethu, A. Sin, M. Toner, *Lab. Chip.* **6**, 83 (2006)
- N. Siegel, M. Rosner, M. Hanneder, A. Freilinger, M. Hengstschläger, *Amino Acids* **35**, 291 (2008)
- C.H. Wang, G.-B. Lee, *J. Micromech. Microeng.* **16**, 341 (2006)
- P. Wilding, L.J. Kricka, J. Cheng, G. Hvichia, M.A. Shoffner, P. Fortina, *Anal. Biochem.* **257**, 95 (1998)
- Z. Wu, A.Q. Liu, K. Hjort, *J. Micromech. Microeng.* **17**, 1992 (2007)
- N. Xia, T. Hunt, B. Mayers, E. Alsberg, G. Whitesides, R. Westervelt, D. Ingber, *Biomed. Microdevices.* **8**, 299 (2006)
- M. Yamada, M. Seki, *Lab. Chip.* **5**, 1233 (2005)
- M. Yamada, M. Nakashima, M. Seki, *Anal. Chem.* **76**, 5465 (2004)
- S.Y. Yang, S.K. Hsiung, Y.C. Hung, C.M. Chang, T.L. Liao, G.B. Lee, *Meas. Sci. Technol.* **17**, 2001 (2006)
- S.Y. Yang, K.Y. Lien, K.J. Huang, H.Y. Lei, G.B. Lee, *Biosens. Bioelectron.* (2008). in press.
- B.L. Yen, H.I. Huang, C.C. Chien, H.Y. Jui, B.S. Ko, M. Yao, C.T. Shun, M.L. Yen, M.C. Lee, Y.C. Chen, *Stem Cells* **23**, 3 (2005)